Iranian Journal of Science and Technology, Transactions A: Science (2019) 43:2651–2655
https://doi.org/10.1007/s40995-019-00708-2

RESEARCH PAPER

Effect of Etching on Nanoporous Anodic Alumina

M. A. Mir[1] · M. A. Shah[1] · P. A. Ganai[2]

Received: 16 August 2018 / Accepted: 2 April 2019 / Published online: 25 April 2019

Abstract
Nanoporous anodic alumina were fabricated by using aqueous oxalic acid electrolyte via the simple and convenient electrochemical anodization method. The pore formation resulted from the interaction of surface aluminum with the prepared electrolyte of 0.3M oxalic acid having pH value less than 5. The phase purity and the morphology of the prepared porous alumina were studied by using X-ray diffraction and scanning electron microscopy respectively. Before pore widening, aluminum oxide nanopores of average pore size ~ 40 nm were obtained. However, after pore widening, nanopores of average pore size ~ 64 nm were obtained. For proper understanding of the formation of porous alumina nanopores, formation mechanism was discussed in detail by using current density–time spectra.

Keywords Aluminum oxide · Oxalic acid · Anodization · Current density–time spectra

1 Introduction

Nanostructures of aluminum oxide show various applications in different areas due to their remarkable properties by virtue of their versatile morphology like nanopores, nanotubes, nanorods, and nanowires. In particular, anodic aluminum oxide has attracted great attention because of its regular and self-organized arrangement into nanopore structures (Chen et al. 2008; Wang et al. 2013; Zaraska et al. 2014; Lee and Park 2014). To fabricate ordered porous structures of aluminum and aluminum oxide, the electrochemical anodization method is one of the convenient and suitable methods. The anodic aluminum oxide (AAO) structures fabricated by this method find applications in advanced research areas such as enhancement in fluid permeation (Kasi et al. 2018), photocatalytic disinfection of contaminated water (Najma et al. 2018), biosensor (Macias et al. 2013), enhancement of fluorescence (Song et al. 2018), solar cells (Wu et al. 2017), enhancement of photoluminescence (An et al. 2018), corrosion resistance (Diggle et al. 1969), surface and structural engineering (Jani et al. 2013), and cancer therapy (Vorozhtsova et al. 2011).

As a result of controllable pore diameter and periodicity, the anodic aluminum oxide (AAO) acts as a template (Bocchetta et al. 2008) and, hence, plays an important role in fabrication of various nanostructures. The structural characteristics of AAO template are determined by anodizing parameters like voltage, anodizing time, anodizing temperature, inter-electrode separation, etc. (Chahrour et al. 2015; Zaraska et al. 2013; Domanska et al. 2018). The homogeneity of the resulting nanostructures depends upon the degree of ordering in nanopores of AAO and thus provides path to synthesize highly ordered nanostructures with high aspect ratio, which is difficult to fabricate through conventional lithographic process (Sulka 2008). Further, the control in the shape and geometry of the nanostructures is important and can be obtained by controlled anodization of aluminum surfaces in aqueous acids like oxalic acid (Lillo and Losic 2009a, b; Romero et al. 2012; Stępniowski and Bojar 2011; Ding et al. 2005; Zhao et al. 2005; Ateş and Baran 2018), sulfuric acid (Lillo and Losic 2009a; Romero et al. 2012; Ono and Masuko 2003), phosphoric acid (Brevnov et al. 2004; Zhang et al. 2010; Zaraska et al. 2010a), etc. Masuda and Fukuda reported the two-step anodization of aluminum which allowed the fabrication of self-ordered AAO structures (Masuda and Fukuda 1995; Masuda and Satoh 1996). In this process, the disordered AAO formed during first anodization was removed to leave periodic concave features on

✉ M. A. Mir
mirphy93@gmail.com

[1] Special Centre for Nano-Science, P. G. Department of Physics, National Institute of Technology, Srinagar, Jammu and Kashmir 190006, India

[2] P. G. Department of Physics, National Institute of Technology, Srinagar, Jammu and Kashmir 190006, India

the surface of aluminum. This nanoconcave structure acts as nucleation sites for pore initiation to obtain highly ordered arrays in the second step of anodization.

The origin and exact mechanism of pore nucleation is not completely known, and to provide deep understanding of the formation mechanism, some models have been put forward. One model explains the formation of pores in aluminum substrate in an electrolyte with pH less than 5, and these pores arise from electric field-assisted chemical dissolution at the electrolyte/oxide interface and oxide generation at the metal/oxide interface (Vrublevsky et al. 2007). Patermarakis (2009) reported that pore formation in aluminum arises on account of recrystallization of the unstable rare lattice of oxide into stable denser nanocrystalline oxide present in the oxide layer. Zaraska et al. (2010b) proposed that rate of oxide growth slows down due to the presence of Al alloy in the sample and also affects structural features like porosity, barrier layer thickness, pore diameter, and pore density of the forming oxide layer. Further, upward growth of the pore wall has recently been explained by Garcia-Vergara et al. (2006), where tungsten tracer was placed in oxide layer formed by the first step of anodization and motion of tracer was monitored, during the second step of anodization, from the metal/oxide interface toward the growing wall structure.

In the present work, anodic aluminum oxide nanopores are fabricated through a mild anodization method in 0.3M oxalic acid at the optimized value of voltage, i.e., 40 V, at room temperature. The structures show well-organized morphology with an average pore diameter of 40 nm. However, after pore widening the average diameter is found to be 64 nm. The formation mechanism of porous structures is analyzed through current density–time spectra. Further, the possible formation mechanism of AAO through dissolution of aluminum, which is governing the growth of porous structure, has been described briefly.

2 Materials

Aluminum foil (99.8% purity), ethanol (C_2H_6O), acetone (C_3H_6O), oxalic acid ($C_2H_2O_4$), phosphoric acid (H_3PO_4), chromic acid (H_2CrO_4), perchloric acid ($HClO_4$), and graphite foil (counter electrode) were brought from Sigma-Aldrich. Further, all the items were of analytical grade and these items were directly used without any further purification.

3 Experiment

Porous structures of aluminum were fabricated by a two-step electrochemical mild anodization technique. The Al foil acted as anode, and graphite foil of the same size was used as a counter electrode (cathode). The annealed aluminum foil having thickness of 0.25 cm was cut into rectangular pieces with dimensions (1 cm × 2 cm). Prior to anodization, the aluminum foil was subsequently degreased ultrasonically in ethanol, acetone, and then in distilled water for 15 min. After sonication, the sonicated aluminum foil was dried for 12 h at room temperature and electrochemically polished under the constant voltage of 10 V in an electrolyte containing mixture of perchloric acid (60 wt%) and ethanol for 1 min. Electro-polished foils were cleaned in de-ionized water and acetone and then allowed to dry at room temperature. The first step of anodization was carried by mounting aluminum foil (sample) in an electrolyte containing 0.3M oxalic acid ($C_2H_2O_4$) under constant stirring and potentiostatic conditions of 40 V at the room temperature for 1 h. An irregular oxide layer on aluminum substrate was removed by immersing the sample in the mixture of 5 wt% phosphoric acid and 2 wt% chromic acid for 1 h at 60 °C. After removal of the irregular oxide layer, Al sample was washed with de-ionized water and acetone and then dried to perform the second step of anodization. The second step of anodization was carried out under the same conditions as in the first step for 30 min. After the second step of anodization, the prepared aluminum sample was immersed in 5 wt% phosphoric acid for widening of nanopores at 30 °C.

The morphology and structural properties of porous anodic alumina were confirmed by using scanning electron microscopy (SEM, HITACHI S-3600N, Japan) and X-ray diffraction techniques (Aeris, Panalytical XRD, using Cu-Kα radiation of wavelength, $\lambda = 0.154$ nm).

4 Results and Discussion

Figure 1 shows X-ray diffraction (XRD) of prepared anodized AAO sample and plane aluminum foil. The XRD spectra of both anodized aluminum and plane aluminum show diffraction peaks at the same value of 2θ; however, intensity of peaks decreases due to anodization.XRD spectra show four characteristic peaks with 2θ values 38.26°, 44.38°, 64.80°, and 77.92° which correspond to (111), (200), (220), and (311) planes of aluminum, respectively, pointing no diffraction peaks of aluminum oxide but only peaks of aluminum. Hence, it is concluded that due to electrochemical anodization, the aluminum foil retains its initial state and did not go through phase transformation.

The first step of anodization in 0.3M oxalic acid for 1 h at room temperature results in the formation of unsymmetrical nanopores. These unsymmetrical nanopores are removed by mounting the anodized aluminum substrate in a mixture of phosphoric acid and chromic acid at 60 °C. The purpose to remove yellowish layer from the first anodized foil is the

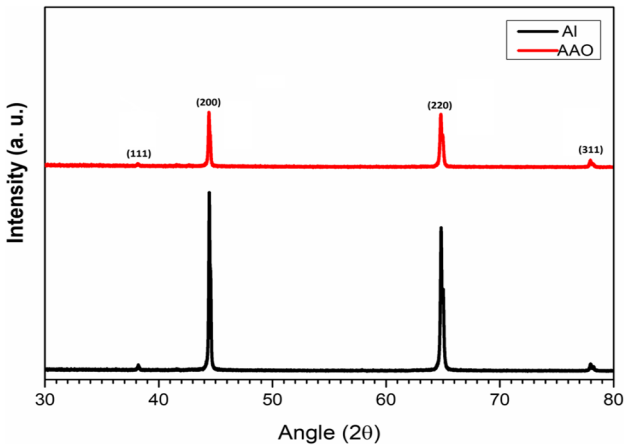

Fig. 1 XRD pattern of plane aluminum foil and anodic aluminum foil

formation of nanoconcave structure on foil which in turn acts as template for the second step.

Figure 2a shows top view of the SEM images of AAO surface after the second step of anodization and Fig. 2b shows top view of AAO after pore widening at different resolution values. Well-defined nanopores with an average pore diameter of nearly 40 nm are obtained through two-step electrochemical mild anodization, and pore widening in phosphoric acid results in the formation of nanopores of average diameter of nearly 64 nm.

During anodization of aluminum, two boundaries are formed. The first boundary is between aluminum metal and oxide formed, and the second boundary is between oxide and electrolyte, i.e., oxide/electrolyte interface (Patermarakis 2009). Initially, when potential difference is created between electrodes the movement of Al^{3+} takes place from the metal through the aluminum/oxide interface (Patermarakis 1998). Simultaneously, movement of O_2^- from water into oxide layer takes place through oxide/electrolyte interface. Most of the Al^{3+} and O_2^- ions combine, which leads to the formation of barrier oxide layer, and the remaining Al^{3+} ions are dissolved into the electrolyte (Shawaqfeh and Baltus 1999). The barrier layer continuously develops, which results in growth of semi-spherical oxide layer of constant thickness which in turn forms the pore bottom.

The anodic aluminum dissolution, which leads to the formation of porous oxide layer, can be written as (Poinern et al. 2011; Naikoo et al. 2015; Naikoo et al. 2014; Dar and Shah 2018a, b):

$$2Al \rightarrow 2Al^{3+} + 6e^-$$

Similarly, the reaction that takes place at the cathode is given as:

$$6H^+ + 6e^- \rightarrow 3H_2$$

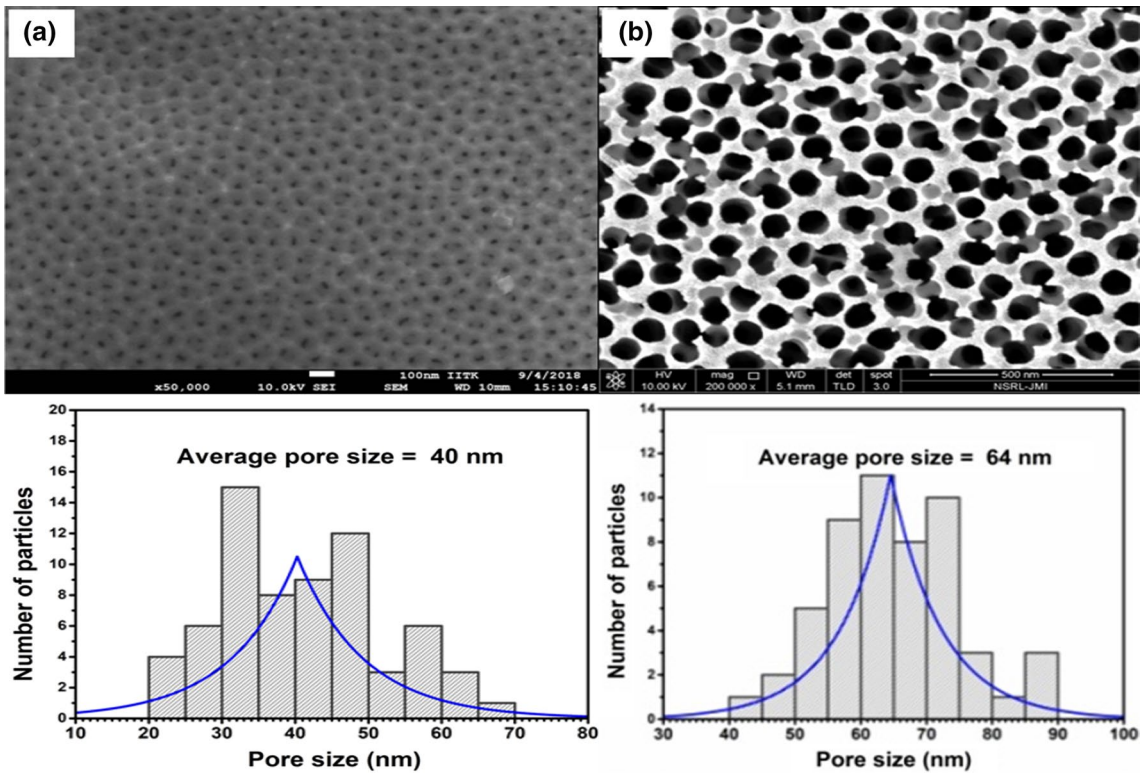

Fig. 2 Top view of AAO: **a** second step of anodization and **b** pore widening

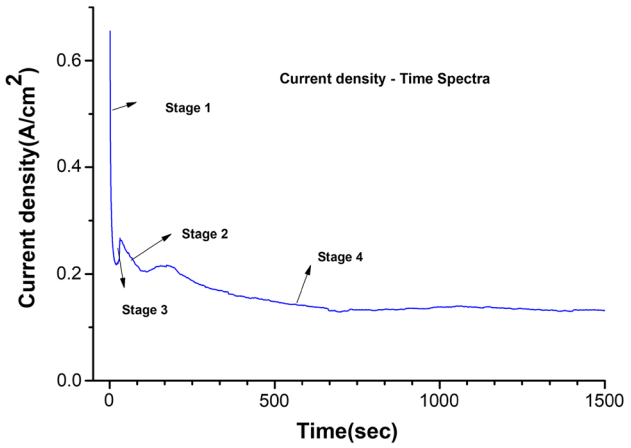

Fig. 3 Current density–time spectra of anodization process

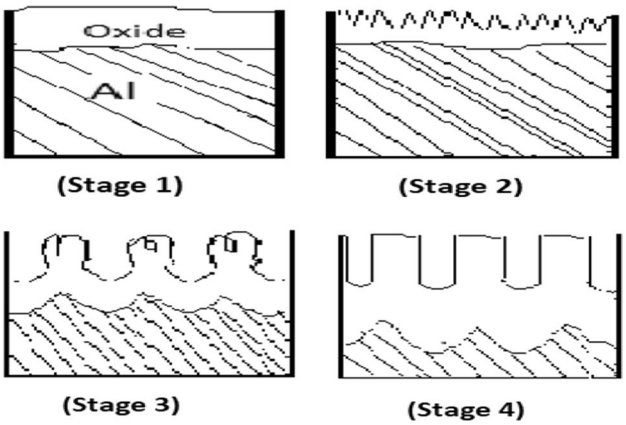

Fig. 4 Schematic diagram of formation porous alumina in potentiostatic conditions

At the aluminum/oxide interface, oxygen anions react with aluminum through the reaction:

$$2Al + 3O_2^- \rightarrow Al_2O_3 + 6e^-$$

Similarly, aluminum ions react with water at the oxide/electrolyte interface as:

$$2Al^{3+} + 3H_2O \rightarrow Al_2O_3 + 6H^+$$

Overall reactions of the anodization process can be represented as:

$$2Al + 3H_2O \rightarrow Al_2O_3 + 3H_2$$

Hence, pore base oxide layer is formed on account of balance between field-assisted oxide dissolution at the oxide/electrolyte interface and the oxide growth at the aluminum/oxide interface.

The formation of porous alumina takes various stages that are observed by monitoring the dependence of current on time under potentiostatic conditions. Graphically, these stages are shown in Fig. 3, and the corresponding possible formation mechanism at different stages is described schematically in Fig. 4. In Stage-1, when bias voltage is switched on, current starts decreasing with time until minima are reached and growth of oxide layer takes place on the surface of Al foil. In Stage-2, current increases and some cracks are exposed, which leads to the formation of pores. In Stage-3, current decreases again and enlargement of cracks is observed through barrier oxide. In Stage-4, current remains almost constant and further anodization results self-assembled and highly ordered porous structure having cylindrical cells and pores at the centers.

5 Conclusion

Anodic aluminum oxide (AAO) porous structures were successfully fabricated through electrochemical anodization method. The following conclusion were drawn: (1) Maintaining pH value of oxalic acid electrolyte less than 5 played a favorable role in the fabrication of porous alumina. (2) The first step of anodization led to the formation of unsymmetrical porous structures of aluminum which acted as template for the second step of anodization. (3) The second step of anodization led to the formation of self-assembled and self-ordered anodic alumina of average pore size of ~40 nm. (4) XRD spectra reveal that aluminum substrate did not experience any phase transformation due to anodization although the intensity of peaks decreases on account of anodization. (5) Current density–time spectra indicate at the final stage current remains constant and is consistent with the theoretical models of mild anodization of aluminum.

Acknowledgements The authors are highly thankful to NIT Srinagar, IIT Kanpur, and Jamia Millia Islamia, New Delhi, for providing experimental facilities.

References

An YY, Wang J, Zhou WM, Jin HX, Li JF, Wang CW (2018) The preparation of high quality alumina defective photonic crystals and their application of photoluminescence enhancement. Superlattices Microstruct 119:1–8

Ateş S, Baran E (2018) The nanoporous anodic alumina oxide formed by two-step anodization. Thin Solid Films 648:94–102

Bocchetta P, Santamaria M, Di Quarto F (2008) Electrosynthesis of Ce–Co mixed oxide nanotubes with high aspect ratio and tunable composition. Electrochem Solid-State Lett 11:K27–K30

Brevnov DA, Barela MJ, Brooks MJ, López GP, Atanassov PB (2004) Fabrication of anisotropic super hydrophobic/hydrophilic

nanoporous membranes by plasma polymerization of C 4 F 8 on anodic aluminum oxide. J Electrochem Soc 151(8):B484–B489
Chahrour KM, Ahmed NM, Hashim MR, Elfadill NG, Maryam W, Ahmad MA, Bououdina M (2015) Effects of the voltage and time of anodization on modulation of the pore dimensions of AAO films for nanomaterials synthesis. Superlattices Microstruct 88:489–500
Chen W, Wu JS, Xia XH (2008) Porous anodic alumina with continuously manipulated pore/cell size. ACS Nano 2(5):959–965
Dar FA, Shah MA (2018a) Low temperature fabrication of Al_2O_3 nanostrips and their enhanced dielectric property. Mater Res Express 5(1):015048
Dar FA, Shah MA (2018b) Structural, morphological and dielectric properties of Li-doped Al_2O_3. Appl Phys A 124(7):513
Diggle JW, Downie TC, Goulding CW (1969) Anodic oxide films on aluminum. Chem Rev 69(3):365–405
Ding GQ, Zheng MJ, Xu WL, Shen WZ (2005) Fabrication of controllable free-standing ultrathin porous alumina membranes. Nanotechnology 16(8):1285
Domanska MM, Stepniowski WJ, Salerno M (2018) Effect of interelectrode separation in the fabrication of nanoporous alumina by anodization. J Electroanal Chem 823:47–53
Garcia-Vergara SJ, Iglesias-Rubianes L, Blanco-Pinzon CE, Skeldon P, Thompson GE, Campestrini P (2006) Mechanical instability and pore generation in anodic alumina. In: Proceedings of the Royal Society of London A: mathematical, physical and engineering sciences, vol 462, no 2072. The Royal Society, London, pp 2345–2358
Jani AMM, Losic D, Voelcker NH (2013) Nanoporous anodic aluminium oxide: advances in surface engineering and emerging applications. Prog Mater Sci 58(5):636–704
Kasi AK, Kasi JK, Bokhari M (2018) Fabrication of mechanically stable AAO membrane with improved fluid permeation properties. Microelectron Eng 187:95–100
Lee W, Park SJ (2014) Porous anodic aluminum oxide: anodization and templated synthesis of functional nanostructures. Chem Rev 114(15):7487–7556
Lillo M, Losic D (2009a) Ion-beam pore opening of porous anodic alumina: the formation of single nanopore and nanopore arrays. Mater Lett 63(3–4):457–460
Lillo M, Losic D (2009b) Pore opening detection for controlled dissolution of barrier oxide layer and fabrication of nanoporous alumina with through-hole morphology. J Membr Sci 327(1–2):11–17
Macias G, Hernández-Eguía LP, Ferré-Borrull J, Pallares J, Marsal LF (2013) Gold-coated ordered nanoporous anodic alumina bilayers for future label-free interferometric biosensors. ACS Appl Mater Interfaces 5(16):8093–8098
Masuda H, Fukuda K (1995) Ordered metal nanohole arrays made by a two-step replication of honeycomb structures of anodic alumina. Science 268(5216):1466–1468
Masuda H, Satoh M (1996) Fabrication of gold nanodot array using anodic porous alumina as an evaporation mask. Jpn J Appl Phys 35(1B):L126
Naikoo GA, Dar RA, Khan F (2014) Hierarchically macro/mesostructured porous copper oxide: facile synthesis, characterization, catalytic performance and electrochemical study of mesoporous copper oxide monoliths. J Mater Chem A 2(30):11792–11798
Naikoo GA, Dar RA, Thomas M, Sheikh MUD, Khan F (2015) Hierarchically porous metallic silver monoliths: facile synthesis, characterization and its evaluation as an electrode material for supercapacitors. J Mater Sci: Mater Electron 26(4):2403–2410
Najma B, Kasi AK, Kasi JK, Akbar A, Bokhari SMA, Stroe IR (2018) ZnO/AAO photocatalytic membranes for efficient water disinfection: synthesis, characterization and antibacterial assay. Appl Surf Sci 448:104–114
Ono S, Masuko N (2003) Evaluation of pore diameter of anodic porous films formed on aluminum. Surf Coat Technol 169:139–142
Patermarakis G (1998) Development of a theory for the determination of the composition of the anodizing solution inside the pores during the growth of porous anodic Al_2O_3 films on aluminium by a transport phenomenon analysis. J Electroanal Chem 447(1–2):25–41
Patermarakis G (2009) The origin of nucleation and development of porous nanostructure of anodic alumina films. J Electroanal Chem 635(1):39–50
Poinern GEJ, Ali N, Fawcett D (2011) Progress in nano-engineered anodic aluminum oxide membrane development. Materials 4(3):487–526
Romero V, Vega V, García J, Prida VM, Hernando B, Benavente J (2012) Ionic transport across tailored nanoporous anodic alumina membranes. J Colloid Interface Sci 376(1):40–46
Shawaqfeh AT, Baltus RE (1999) Fabrication and characterization of single layer and multi-layer anodic alumina membranes. J Membr Sci 157(2):147–158
Song M, Zhou X, He X, Cao H, Liu J, Qiu H, Jin Z (2018) Distance dependent fluorescence enhancement of silver nanowires deposited on AAO. Opt Mater 83:241–244
Stępniowski WJ, Bojar Z (2011) Synthesis of anodic aluminum oxide (AAO) at relatively high temperatures. Study of the influence of anodization conditions on the alumina structural features. Surf Coat Technol 206(2–3):265–272
Sulka GD (2008) Highly ordered anodic porous alumina formation by self-organized anodizing. Nanostruct Mater Electrochem 1:1–116
Vorozhtsova M, Drbohlavova J, Hubalek J (2011) Chemical microsensors with ordered nanostructures. In: Microsensors. https://doi.org/10.5772/18066
Vrublevsky I, Jagminas A, Schreckenbach J, Goedel WA (2007) Electronic properties of electrolyte/anodic alumina junction during porous anodizing. Appl Surf Sci 253(10):4680–4687
Wang Q, Long Y, Sun B (2013) Fabrication of highly ordered porous anodic alumina membrane with ultra-large pore intervals in ethylene glycol-modified citric acid solution. J Porous Mater 20(4):785–788
Wu L, Zhang H, Qin F, Bai X, Ji Z, Huang D (2017) Performance enhancement of pc-Si solar cells through combination of antireflection and light-trapping: functions of AAO nano-grating. Opt Commun 385:205–212
Zaraska L, Sulka GD, Jaskuła M (2010a) The effect of n-alcohols on porous anodic alumina formed by self-organized two-step anodizing of aluminum in phosphoric acid. Surf Coat Technol 204(11):1729–1737
Zaraska L, Sulka GD, Szeremeta J, Jaskuła M (2010b) Porous anodic alumina formed by anodization of aluminum alloy (AA1050) and high purity aluminum. ElectrochimicaActa 55(14):4377–4386
Zaraska L, Stępniowski WJ, Ciepiela E, Sulka GD (2013) The effect of anodizing temperature on structural features and hexagonal arrangement of nanopores in alumina synthesized by two-step anodizing in oxalic acid. Thin Solid Films 534:155–161
Zaraska L, Stępniowski WJ, Jaskuła M, Sulka GD (2014) Analysis of nanopore arrangement of porous alumina layers formed by anodizing in oxalic acid at relatively high temperatures. Appl Surf Sci 305:650–657
Zhang R, Jiang K, Ding G (2010) Surface morphology control on porous anodic alumina in phosphoric acid. Thin Solid Films 518(14):3797–3800
Zhao Y, Chen M, Zhang Y, Xu T, Liu W (2005) A facile approach to formation of through-hole porous anodic aluminum oxide film. Mater Lett 59(1):40–43